NEW CONCEPT OF MODELING TO PREDICT TEMPERATURE IN OIL-HYDRAULIC CYLINDER CHAMBER CONSIDERING INTERNAL FLOW

Kazuhiro TANAKA[a], Kouki TOMIOKA[b], Masaki FUCHIWAKI[c], Katsuya SUZUKI[d]

[a][c][d]Kyushu Institute of Technology
[b]NITTO DENKO Co.

[a]kazuhiro@mse.kyutech.ac.jp, [b]kouki_tomioka@gg.nitto.co.jp, [c] futiwaki@mse.kyutech.ac.jp,
[d]kachandesu2002@yahoo.co.jp

ABSTRACT

It is important to study a precise and practical way to predict temperature rise of oil hydraulic systems. It is interesting whether internal flow patterns have any effect on temperature change in a cylinder. Nowadays commercial CFD (Computational Fluid Dynamics) codes give accurate solutions of temperature as well as flow patterns. The authors have calculated the flow patterns in a cylinder using a reliable CFD code and have found that three-dimensional effect is very strong there and the internal flow patterns can be classified into two flow regions with 3D vortex flow pattern and 1D parallel flow pattern. So, it becomes possible to predict precisely temperature change in a cylinder by incorporating the internal flow patterns with modeling method based on a lumped parameter system. A new method with prediction of temperature rise in a cylinder is proposed in this study.

Keywords: oil-hydraulic cylinder, temperature prediction, lumped parameter system, vortex flow pattern

1. INTRODUCTION

An oil-hydraulic system has become so compact and highly-pressurized recently. Its small heat capacity or small surface area for heat dissipation causes high temperature rise of a system while it works for long time under highly loaded condition. The high temperature rise causes deterioration of working oil and the system may become dangerous finally. From this viewpoint, it is important to study a precise and practical way to predict system temperature.

In a viewpoint that energy loss causes temperature rise in a system, modeling and simulation by Bondgraph method is very effective to predict the temperature rise because the method is based on energy balance. In the past some studies have been conducted to predict temperature of oil-hydraulic systems considering heat generation and heat transfer in components of the systems. Johansson analyzed heat generation from a hydraulic motor embedded in an aircraft actuator system and heat transfer from oil passages (Johansson et al., 2001). Yamamoto analyzed heat generation and heat transfer from oil circuits of a mobile crane (Yamamoto et al., 1997). Tomioka proposed a new idea to predict temperature rise of a hydraulic pipe by considering heat transfer between working oil and a pipe-housing (Tomioka et al., 2005). In this study, one-dimensional Bondgraph modeling based on a lumped parameter system is applied to predict temperature inside the pipe and three-dimensional heat conduction analysis method is applied to calculate temperature distribution in the pipe-housing. By coupling the above two prediction methods the temperature distribution in the pipe component is well predicted time-dependently.

Following Tomioka's study (Tomioka et al., 2005), a new idea to predict temperature distribution in a cylinder is studied in the present study. While a cylinder works for long time, the temperature distribution appears there. In modeling with a lumped parameter system, it is generally believed that the more dividing number of elements becomes, the more precise calculation results will be obtained. It is interesting whether the idea is applicable to a cylinder or not and whether an internal flow in a cylinder has any effect on the temperature distribution.

Commercial CFD (Computational Fluid Dynamics) codes are developing rapidly accompanied with remarkable developments of computers in recent years. Not only the improvement of analysis precision, but also new functions such as moving body analysis have been introduced and sophisticated. The authors have calculated internal flow patterns in a cylinder using a reliable CFD code and have found that three-dimensional effect is very strong there. However, a prediction of time-dependent temperature change is not practical because the calculations with CFD codes are much time-consuming.

In this study, internal flow patterns in an oil-hydraulic cylinder has been calculated and verified that the flow patterns can be classified into two flow regions with 3D vortex flow pattern and 1D parallel flow pattern. So, it becomes possible to predict precisely the temperature distribution in the cylinder by incorporating the internal flow patterns with modeling based on a lumped parameter system.

NOMENCLATURE

A [m^2] heat dissipation surface area of cylinder
a [m] representative length of inlet head port
b [m] length from cylinder end to inlet port center
c_p [J/kgK] specific heat at constant pressure
D [m] cylinder diameter
E [J] internal energy
H [J] enthalpy
h [W/m^{2}K] heat transfer coefficient
Lx [m] location of dividing between 3D and 1D flow
N [s] reciprocating motion cycle of piston
P [Pa] pressure
Q [m^3/s] volumetric flow rate
R_c [m] standard diameter of inlet head port
$\dot{q}$ [W] amount of heat inflow
T [K] temperature
t [s] time
$\mathbf{U}$ [m/s] velocity vector
V [m^3] volume of cylinder head chamber
v [m/s] velocity
W [W] power consumed for outside
x [m] axial location of piston head
δ [-] Kronecker delta
λ [W/mK] thermal conductivity
μ [Pas] viscous coefficient
ν [m^2/s] kinematic viscous coefficient
ρ [kg/m^3] density

Suffix
c cylinder
in inflow
p piston
$1D$ one-dimensional
$3D$ three-dimensional

2. NUMERICAL SIMULATION METHOD

2.1. One-dimensional Model of Heat Balance

Figure 1 shows a schematic figure of heat balance in a cylinder. Temperature in a cylinder chamber is calculated as the sum of amount of heat inflow and outflow of working oil, volumetric change of working oil, and heat dissipation to cylinder housing. First law of thermodynamics derived the following equation.

$$\frac{dE}{dt} = \frac{dH}{dt} + \dot{q} - W \tag{1}$$

If pressure loss of working oil could be negligibly-small in the inlet and outlet port and working oil does not work against outside, changing rate of the internal energy is expressed by the following equation.

$$\frac{dE_c}{dt} = c_p \rho Q T_i + h A_c \left(T_{wall} - T_c \right) \tag{2}$$

$$if \quad Q \geq 0 (in) \; T_i = T_{in}$$
$$Q \leq 0 (out) \; T_i = T_c$$

When the cylinder volume changes time-dependently with piston motion the changing rate of internal energy is expressed by the following equation.

$$\frac{dE_c}{dt} = c_p \rho \frac{dV_c T_c}{dt} = c_p \rho \left(T_c \frac{dV_c}{dt} + V_c \frac{dT_c}{dt} \right) \tag{3}$$
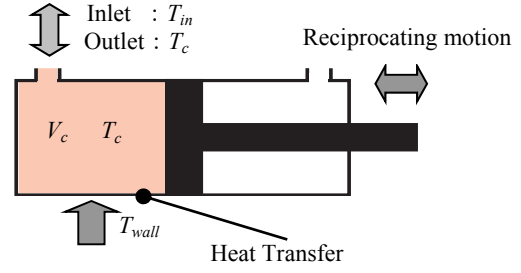

Figure 1: Heat Balance in Cylinder

Equation (4) is derived from Eq. (2) and Eq. (3) in the cylinder chamber.

$$\frac{dT_c}{dt} = \frac{1}{c_p \rho V_c} \left\{ c_p \rho Q T_i + h A_c \left(T_{wall} - T_c \right) - c_p \rho T_c \frac{dV_c}{dt} \right\} \tag{4}$$

In the above equation, the first term of right hand side indicates the inflow or outflow amount of heat with piston motion, the second term the amount of heat transfer between the cylinder chamber and cylinder housing, and the third term the effect of cylinder volume change. The temperature in the cylinder chamber can be calculated by solving Eq. (4) using Runge-Kutta method.

2.2 Governing Equations in CFD Calculations

A commercial CFD code, ANSYS-CFX(ANSYS, 2005) which is world-widely used today and gives reliable results even in case of moving bodies, is used to analyze flow patterns as well as temperature distribution time-dependently in a hydraulic cylinder in the present study. However, time-dependent CFD calculations consume so much time that the calculating method is not practical for system simulations despite giving precise results. In the present study the validity of temperature prediction method proposed as one-dimensional modeling method based on a lumped parameter system (hereafter 1D-Model) is verified by comparing numerical results obtained through three dimensional analyses with a CFD code (hereafter 3D-CFD).

The flow patterns as well as heat transport phenomena are solved using the following equations, where Eq. (5) is equation of continuity, Eq. (6) Navier-Stokes equation, and Eq. (7) energy equation.

$$\frac{\partial \rho}{\partial t} + \nabla \bullet (\rho U) = 0 \tag{5}$$

$$\frac{\partial \rho U}{\partial t} + \nabla \bullet (\rho U \otimes U) = \nabla \bullet \left(-P\delta + \mu \left(\nabla U + (\nabla U)^T \right) \right) \tag{6}$$

$$\frac{\partial \rho H}{\partial t} - \frac{\partial P}{\partial t} + \nabla \bullet (\rho U H) = \nabla \bullet (\lambda \nabla T) \tag{7}$$

The discretization way of the above equations is based on finite volume method and hexahedrally-bonded structured grid is generated as a numerical grid system.

3. CHARACTERISTICS OF 1D-MODEL

3.1. Analysis Conditions

In order to study characteristics of Eq. (4), a simple system shown in Fig. 2 is firstly set as an example model. This model indicates a piston head chamber of a

double-acting cylinder. The cylinder diameter is 100 mm, the initial length of the chamber 500 mm and the head port with rectangular configuration 10×10 mm². The pressure at the head port is set as 0 Pa as the boundary condition and the piston is moved along sine function with motion frequency 0.1 Hz and amplitude 100 mm. The initial temperature in the chamber is set 20 deg. as the initial condition and the temperature of working oil inflow is always set 40 deg. In the present study, cylinder walls are set adiabatic not to consider interference between the chamber inside and the cylinder housing but to consider energy balance only in the chamber inside. The grid number for 3D-CFD calculation is 61,000 nodes and 57,000 elements which is enough to calculate unsteady flow patterns as well as heat transport phenomena. The analysis conditions and properties of the working oil are shown in Table 1.

3.2. Results

Figure 3 shows the comparison between 1D-Model calculation and 3D-CFD simulation on the cylinder temperature. The horizontal axis indicates time and the vertical axis temperature of working oil in the cylinder chamber. The broken line indicates volume-average temperature of 3D-CFD simulation using Eq. (5)-(7) and the solid line the calculated temperature based on 1D-Model using Eq. (4). At inflow of working oil from Time=7.5 to Time=12.5, the temperature rise is almost same between 1D-Model calculations results and 3D-CFD results. However, at outflow of working oil from Time=12.5 to Time=17.5, the temperature obtained in 3D-CFD simulations decreases despite the constant temperature obtained in 1D-Model calculations.

This is because heat amount of working oil inflow is simultaneously diffused in the chamber and the inside temperature is fixed to the average temperature in 1D-Model and the temperature is kept constant there at outflow of working oil. On the other hand, in the results of 3D-CFD simulations at inflow the working oil with high temperature stays near head port and at outflow the working oil with high temperature flows out first and as a result the volume-average temperature in the chamber decreases. This difference of mechanism causes the error of 1D-Model. It is verified that the prediction precision of result based on Eq. (4) is not enough and the model should be improved to predict the chamber temperature more precisely.

3.3. Effect of Dividing Number of Elements in 1D-Model

In order to improve precision of temperature prediction based on 1D-Model lumped parameter system, cylinder chamber is divided into some partial elements in axial direction, as shown in Fig. 4. The effect of dividing number of elements is studied in case of 3, 5 and 10 divisions. The element volume is time-dependently changed at the element, which corresponds to amplitude of piston motion, and the temperature change is expressed by the last term of Eq. (4).
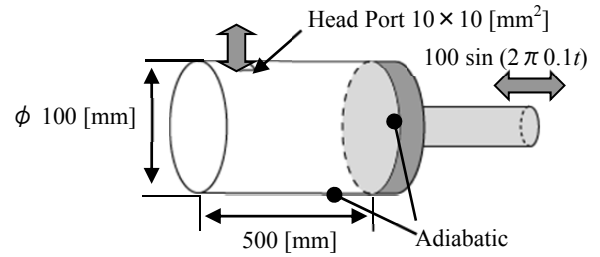
Figure 5 shows the result of comparison on the

Figure 2: Test Model for Cylinder

Table 1: Analysis Conditions

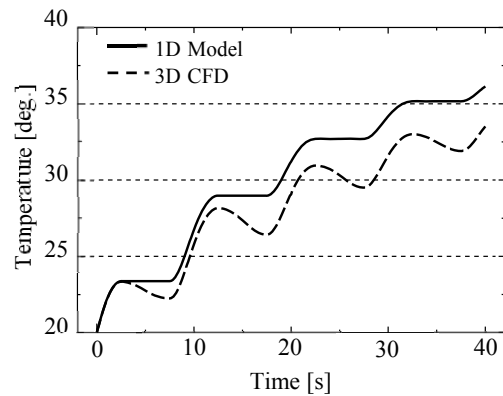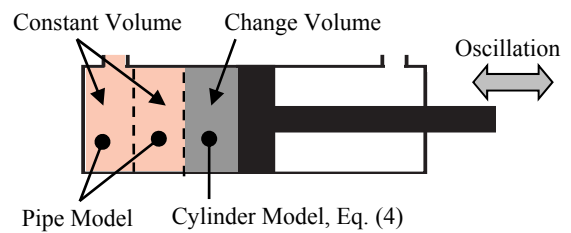| Physical Properties	ρ =860 [kg/m³], μ =0.027 [Pas] λ =0.13[W/mK], c_p=1894 [J/kgK]
Turbulence Model	SST (Shear Stress Transport)[5]
Time Step	1D (Eq. (4)) : 1.0×10^{-5} [s]
	3D (CFD) : 1.0×10^{-2} [s]
Boundary Conditions	Inlet : T_{in} = 40 [deg.], P=0.0 [Pa] Wall : Adiabatic, Non-Slip Wall
Cylinder Motion (sin wave)	Frequency :0.1 [Hz] Amplitude :100 [mm]

Figure 3: Temperature Change at Cylinder

Figure 4: Divide Model for Cylinder (3 Divisions)

volume-average temperature of cylinder between the results in 1D-Model with 3, 5 and 10 divisions and the results in 3D-CFD simulation. The prediction becomes more precise. However, Fig. 5 shows strange tendency. The more precise the prediction becomes, the more the dividing number increases in case of 3 and 5 divisions. However, the difference from 3D-CFD results increases inversely in case of 10 divisions.

$$Error = \frac{1}{2N} \int_0^{2N} \frac{|T_{3D} - T_{1D}|}{T_{3D}} dt \qquad (8)$$

Here the inverse tendency is discussed. The difference between 1D-Model and 3D-CFD results is represented as the error defined in Eq. (8), where N, T_{3D} and T_{1D} indicate the piston motion cycle, the temperature predicted through 3D-CFD simulation, and the temperature predicted through 1D-Model calculation, respectively.

Figure 6 shows relationship between the error and the dividing numbers of elements in modeling of the cylinder. The error reaches a minimum at 6 divisions; however the error becomes higher as the dividing numbers of elements increases. Figure 7 shows a 3D-CFD result of the streamlines through the inlet port in the cylinder chamber when the piston is moving with the maximum speed at neutral position, x = 0 mm, from the maximum displacement, x = -100 mm. In this figure three arrows are described at intervals of 100 mm from the cylinder head end. 3D vortex flow is strongly generated near the inlet port and the flow becomes like parallel as the working oil flows further. Here it can be possible to classify the flow field in the cylinder chamber into two parts, one of which is 3D vortex flow region and another 1D parallel flow region. In the 3D vortex flow region the temperature distribution is so complicated and non-uniform by the vortex flow that the error becomes higher when the region with 3D vortex flow is automatically divided into some elements like the parallel flow region. Consequently the manner to divide automatically the region with complex flow pattern into some elements with the same volume causes imprecise prediction.

4. IMPROVEMENT OF CYLINDER 1D-MODEL

Here a new modeling concept is introduced to improve the 1D-Model of a cylinder based on lumped parameter model. The concept is that the region with 3D vortex flow should be separated from the region with 1D parallel flow in the modeling. Figure 7 shows an internal flow pattern inside a cylinder obtained by 3D-CFD calculation. The figure shows that a transition region between 3D vortex flow and 1D parallel flow can be seen near x= 200 mm, which is called Location of Dividing flow patterns (hereafter LoD).

Figure 8 shows the result obtained when 3D vortex flow region is modeled as one element and 1D parallel flow region is divided into 3, 5 and 10 elements. As the dividing number of elements increases, the result of 1D model asymptotically approaches 3D-CFD calculation results. As a result, it is verified that in order to obtain precise prediction using a lumped parameter system, it is better not to divide total region of a cylinder into elements automatically but to model 3D-vortex flow region as one element and the other region as some elements.

Figure 9 shows the relationship between the prediction error and the dividing number of elements when LoD is set different locations. When LoD is set x= 200 mm, the error is minimum at the respective dividing number of elements. This result means that it is important for precise prediction to set LoD suitably by comparing with 3D-CFD calculation results.
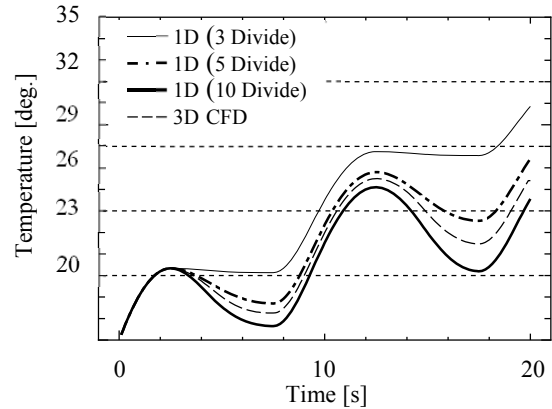
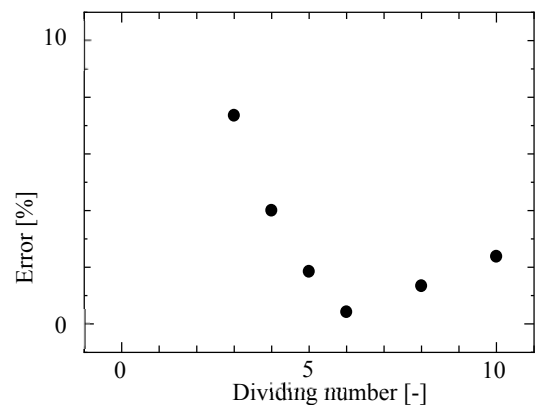Figure 5: Results of 3D-CFD and 1D Analysis

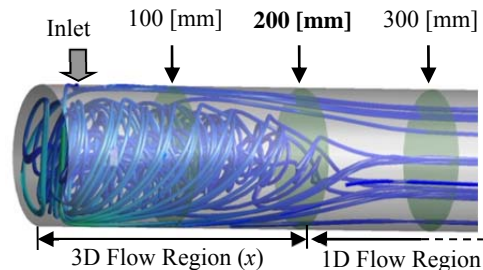Figure 6: Prediction Error of Temperature at Cylinder
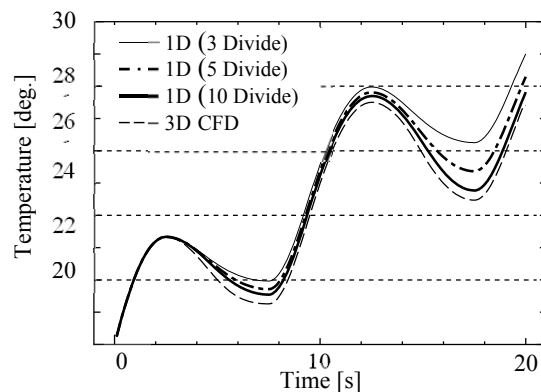
Figure 7: Streamlines at Cylinder Chamber

Figure 8: Temperature Change at Cylinder

5. GENERALIZATION OF NEW 1D-MODEL OF A CYLINDER

It is important to determine the size of 3D vortex flow region in order to set suitable LoD for precise prediction. However, because cylinder size as well as the properties of working oil change the suitable LoD, it is inevitable to generalize the way to determine LoD in order to apply the proposed model to any cylinder. Here generalization of the way to determine LoD has been performed through dimensional analyses considering directional dependency against any cylinder with a different size. The size of 3D vortex flow region may depend on the piston speed. Here it is supposed that the piston speed is constant when the piston moves from piston head side to rod side. Table 2 shows calculating conditions.

Figure 10 shows the maximum vorticity of rotation about the cylinder axis at any axial length from the cylinder head end. In this study, LoD is defined as the length from the cylinder head end to the location with 95% down of the maximum vorticity.

All of parameters affecting on LoD are shown in Fig. 11. Considering directional effects in this study, dimension of length in each direction is defined as $[L_x]$, $[L_y]$ and $[L_z]$ in three dimensional coordinate system. A cylinder diameter, piston velocity, velocity of inlet flow, length of inlet port, and length from the cylinder head end to the center of the inlet port are defined as D, $[L_z]$, v_p $[L_x/s]$, v_{in} $[L_z/s]$, a $[L_x]$, and b $[L_x]$, respectively. The viscous coefficient and the density are selected as the important parameters of the properties of working oil. They are defined as μ $[kgL_z/L_xL_ys]$ and ρ $[kg/L_xL_yL_z]$, respectively.

Through Buchingham's π theorem, the following equation is derived from these parameters.

$$F\left(\frac{D}{a}\cdot\frac{\rho D v_p}{\mu}, \frac{\rho D v_{in}}{\mu}, \frac{b}{a}, \frac{x}{a}\right)=0 \qquad (9)$$

In the above equation, the non-dimensional length of LoD expressed by x/a is a function of Reynolds number expressed by $\rho D v_{in}/\mu$ with representative velocity v_{in}, the product of Reynolds number with representative velocity v_p and D/a, and the non-dimensional length b/a. After determining unknown parameter values so that LoD is the same as the result of 3D-CFD calculations, the following characteristic equations are derived crossing the dividing line of $\rho D v_{in}/\mu =2.3\times10^4$.

LoD [x/a]:
(ⅰ) $\rho D v_{in}/\mu \geq 2.3\times10^4$

$$\frac{x}{a}=1.44\left(\frac{D}{a}\cdot\frac{\rho D v_p}{\mu}\right)^{-0.014}\left(\frac{\rho D v_{in}}{\mu}\right)^{0.19}\left(\frac{b}{a}\right)^{0.27} \qquad (10)$$

(ⅱ) $\rho D v_{in}/\mu < 2.3\times10^4$

$$\frac{x}{a}=0.015\left(\frac{D}{a}\cdot\frac{\rho D v_p}{\mu}\right)^{-0.69}\left(\frac{\rho D v_{in}}{\mu}\right)^{0.96}\left(\frac{b}{a}\right)^{0.098} \qquad (11)$$

Figure 12 shows the comparison of LoD obtained between through the above characteristic equations and through 3D-CFD calculations. The abscissa and ordinate indicate Reynolds number with representative
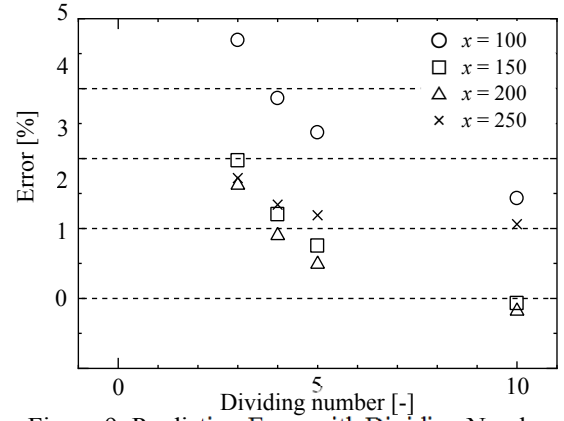
Figure 9: Prediction Error with Dividing Number

Table 2: Conditions for Dimensional Analysis

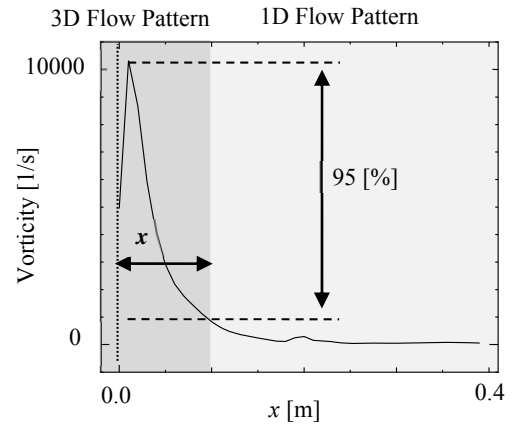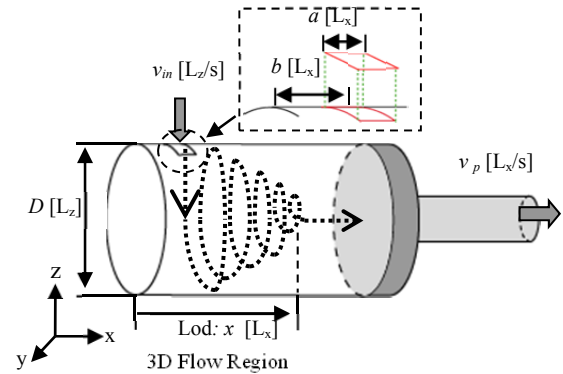| Cylinder Diameter	D=0.07, 0.1, 0.15 [m]
Piston Velocity	V_p= 0.05, 0.1, 0.15 [m/s]
Kinematic Viscosity	32×10^{-6}, 11.5×10^{-6} [m²/s]

Figure 10: Definition of LoD

Figure 11: Parameters of Dimension Analysis

velocity v_{in} and the non-dimensional length LoD [x/a], respectively. The maximum difference is 14% and the both results agree well. It is verified that the suitable LoD for precise prediction can be calculated through the above characteristic equations. Moreover, even when the shape of inlet port is round the results are almost the same as the above results in case of rectangular inlet port by setting inlet port diameter as the representative length, a.

Figure 13 shows applicability of Eq. (10) and (11) to any cylinder contained in a catalogue of products (TAIYO, LTD, 2005). The abscissa and ordinate indicate cylinder diameter D and non-dimensional diameter of inlet port R_c/D, respectively. LoD of all practical products contained in the catalogue (Series A, B and C, TAIYO, LTD, 2005) can be represented well by the above equations. It is verified that the above equations can be applicable to any practical cylinder.

Table 3 shows comparison of calculating time between in 1D-Model calculation proposed in this study and in 3D-CFD calculation. In case of calculating temperature distributions inside a cylinder for practical 20 seconds, 1D-Model calculation takes only 10 [s] though 3D-CFD calculation takes $1.9 \times 10^{+5}$[s]. The difference of volume-average temperature of cylinder chamber between 1D-Model analysis according to Eq. (10) and (11) and 3D-CFD calculation is about 1% and precise prediction can be obtained successfully.

6. CONCLUSIONS

1D-Model predicting temperature of cylinder chamber is proposed and its applicability to any cylinder is verified by comparing with 3D-CFD calculation results.

(1) In a cylinder chamber, inflow generates 3D vortex flow region near the inlet port and does not mix with working oil previously fulfilled. And parallel flow region appears near a piston head. The working oil at this 3D vortex region flows out first at delivery time. When a piston moves with reciprocating motion, temperature has its distribution in axial direction inside a cylinder chamber and it becomes different from volume-average temperature.

(2) In modeling cylinder chamber based on a lumped parameter system in order to predict axial distribution of temperature, it is important to divide 3D vortex flow region and parallel flow region like 1D flow. If the 3D vortex flow region is divided automatically into some elements with the same volume, it may cause imprecise prediction. Inversely modeling 3D-vortex flow region as only one element and dividing another region like 1D parallel flow into some elements give precise prediction of temperature in a cylinder chamber.

(3) Dimensional analysis derives the characteristic equations to determine the suitable length of Location of Dividing between 3D vortex flow region and parallel flow region. The prediction model based on a lumped parameter system by use of Location of Dividing gives quickly simulation results close to 3D-CFD calculation results. The characteristic equations on Location of Dividing proposed in this study are applicable to any practical product.

REFERENCES

ANSYS, 2005, *ANSYS CFX-Solver, Release 10.0.*

Johansson, B., Anderson, J., Krus, P., 2001. Thermal Modeling of an Electro-Hydrostatic Actuation System,*Proceedings of the International Conference on Recent Advantages in Aerospace Actuation System and Components*, Toulouse, France.
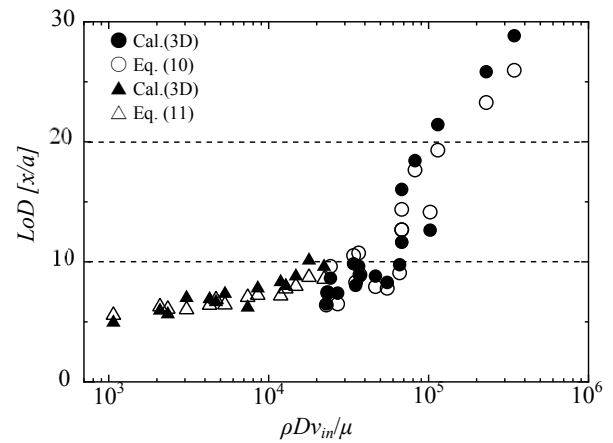
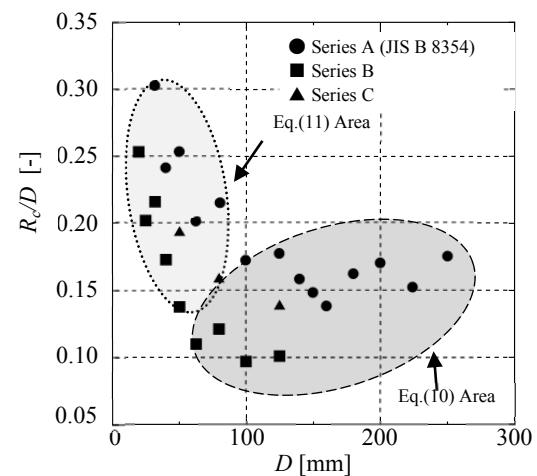Figure 12: Non-dimensional Directional Analysis

Figure 13: Area of Prediction Equation

Table 3: Calculation Time and Error

CPU Power	Calculation Time		Error
Pentium Xeon 3.6 GHz	1D Analysis	10 [s]	1 [%]
	3D-CFD	$1.9 \times 10^{+5}$ [s]	

Menter, F. R., 1994, Tow-Equation Eddy-Viscosity Turbulence Model for Engineering Applications, *AIAA JOURNAL*, **32**-8, 1598-1605.

Tomioka, K., Tanaka, K., Nagayama, K., Tokuda, K., 2005. Prediction method of heat generation and heat transfer in an oil-hydraulic system, *Proc. of IMAACA2005*, 89-94.

TAIYO, LTD, 2005, Products, Hydraulic Equipment, *http://www.taiyo-ltd.co.jp/eg/index.html.*

Yamamoto, K., Tanaka, K., Nakanishi, M., Tarumi, S., 1997, Analysis of Dynamic Behavior of a Hydraulic and Pneumatic Suspension Including Temperature Change Effect, *Proc. of 5th Tri. Int. Symp. on Fluid Control, Measurement and Visualization (FLUCOME97)*, Vol. 1, 457-462.